Biogeosciences Discuss., 4, 69–98, 2007
www.biogeosciences-discuss.net/4/69/2007/

Biogeosciences Discussions

Biogeosciences Discussions is the access reviewed discussion forum of *Biogeosciences*

Carbon isotope fractionation in developing natural phototrophic biofilms

M. Staal[1,*], R. Thar[2], M. Kühl[2], M. C. M. van Loosdrecht[3], G. Wolf[3], J. F. C. de Brouwer[1], and J. W. Rijstenbil[1]

[1]Department of Marine Microbiology, Netherlands Institute of Ecology – KNAW, P.O. Box 140, 4400 AC Yerseke, The Netherlands
[2]Marine Biological Laboratory, Institute of Biology, University of Copenhagen, Strandpromenaden 5, 3000 Helsingør, Denmark
[3]Department of Environmental Biotechnology, TU Delft, Julianalaan 67, 2628 BC Delft, The Netherlands
[*]now at: Department of Environmental Biotechnology, TU Delft, Julianalaan 67, 2628 BC Delft, The Netherlands

Received: 8 January 2007 – Accepted: 16 January 2007 – Published: 24 January 2007

Correspondence to: M. Staal (staal.marc@gmail.com)

Abstract

Natural phototrophic biofilms are influenced by a broad array of abiotic and biotic factors and vary over temporal and spatial scales. Different developmental stages can be distinguished and growth rates will vary due to the thickening of the biofilm, which are expected to lead to a limitation of light or mass transport. In this study it is shown that a variation of the availability of CO_2 leads to a shift in fractionation, thereby affecting $\delta^{13}C$ signatures during the successive developmental stages. For phototrophic freshwater biofilms it was found that the $\delta^{13}C$ value became less negative with the thickening of the biofilm, while the opposite trend in $\delta^{13}C$ values was found in marine biofilms. Modeling and pH profiling indicated that the change in the freshwater system was caused by an increase in CO_2 limitation resulting in an increase of HCO_3^- as C-source. The opposite trend in the marine system could be explained by a higher heterotrophic biomass and activity causing a higher carbon recycling and thereby lower $\delta^{13}C$ values. We conclude that $\delta^{13}C$ was more related to the net areal photosynthesis rate and carbon recycling, rather than to the growth rate of the biofilms.

1 Introduction

Phototrophic biofilms are surface-associated microbial communities, in which the major source of energy and biomass originates from microalgae and bacteria. They thrive on submerged biotic or abiotic substrata in light-exposed aquatic environments and exo-biopolymers (mostly polysaccharides) provide adhesion and cohesion to the microbial consortia in these biofilms (Decho, 2000). During the initial phase of biofilm development the maximum growth rate is determined by the incident irradiance, since at that stage the biofilm thickness does not limit diffusive transport of any of the substrates. Eventually, with the thickening of a biofilm both light attenuation and diffusive transport will progressively become limiting factors for growth. Diffusion limitation will increase during the development of a biofilm due to an increased biovolume-to-surface ratio,

BGD
4, 69–98, 2007

while the potential volumetric enzymatic rates remain equal. At high irradiances mass transfer eventually determines the maximum thickness of a biofilm.

Phototrophic biofilms grow in all aquatic systems ranging from fresh water to hyper saline and all oxygenic phototrophs use RUBISCO in their photosynthetic apparatus for carbon fixation, and the inorganic carbon source used by RUBISCO is $CO_{2(aq)}$. One difference in chemistry between freshwater- and marine systems is that the latter mostly posses a stronger carbonate buffering and therefore mostly have higher inorganic carbon contents (Stumm and Morgan 1995). This results in a higher pH and a dominance in bicarbonate concentration relative to $CO_{2(aq)}$. In marine systems the dissolved inorganic pool consists of dissolved CO_2 (<1%), HCO_3^- (~95%), and CO_3^{2-} (~5%). Due to the low CO_2 concentration and a slow chemical conversion rate of HCO_3^- to CO_2, the supply of CO_2 may therefore be considered as a potentially limiting factor. On the other hand, high respiration rates of heterotrophic and phototrophic organisms present in biofilms, may elevate the $CO_{2(aq)}$ levels and as a result lower the pH.

The inorganic carbon pool available for phototrophs consists of carbon atoms with different atomic weights, mainly ^{12}C (~99%) and ^{13}C (~1%) (Raven, 1998). Organic carbon in phototrophic organisms is generally depleted in ^{13}C relative to the carbon source. This depletion is caused by a biological fractionation due to an enzymatic discrimination against ^{13}C in the photosynthetic process (Hayes, 1993). Under non-limiting conditions, fractionation by RUBISCO results in a $\delta^{13}C$ ranging from –29‰ in plants to –21‰ in cyanobacteria (Roeske and O'Leary, 1985); eukaryotic algae have RUBISCO fractionation values intermediate of these (Lewis et al., 2000). However, the overall fractionation of $\delta^{13}C$ in photosynthetic biofilms is not only the result of the biochemical properties of RUBISCO, but is also affected by CO_2 limitation within the biofilm, which will lower the effective enzymatic fractionation of RUBISCO for two reasons: firstly, the competition between both substrates $^{13}CO_2$ and $^{12}CO_2$ for the binding sites in RUBISCO becomes less as the diffusive transport becomes more important for the CO_2 binding rate to the enzyme; it can be assumed that the diffusive transport rate is equal for both substrates. Secondly, discrimination against ^{13}C will mostly lead to

BGD
4, 69–98, 2007

a ^{13}C enrichment of the remaining $CO_{2(aq)}$ pool. A shift in isotopic composition of the dissolved inorganic carbon (DIC) pool will result in an additional change in $\delta^{13}C$ of the organic material since fractionation (ε_p) is independent of the $\delta^{13}C$ from the source (Lewis et al., 2000; Werne and Hollander, 2004; Hayes, 1993).

Many algae can increase the conversion rate of HCO_3^- to $CO_{2(aq)}$ by the enzyme carbonic anhydrase (CA) (Tortell and Morel, 2002; Cassar et al., 2004) and thereby increase the availability of CO_2 for RUBISCO. This enzyme catalyzes the hydration and dehydration of CO_2. The presence of CA activity in phototrophic biofilms will influence the $\delta^{13}CO_{2(aq)}$ and can increase the incorporated $\delta^{13}C$ up to 10‰ (Goericke et al., 1994).

Most studies on $\delta^{13}C$ in photosynthetic microorganisms focus on phytoplankton species and it is found that $\delta^{13}C$ values of cultured marine phytoplankton species vary from –30‰ to –18‰, while freshwater phytoplankton ranges $\delta^{13}C$ between –40‰ to –25‰. The $\delta^{13}C$ values do not only vary amongst species (Lewis et al., 2000), they also vary within species due to environmental factors such as growth rate, pH of the medium (i.e. $CO_{2(aq)}$ availability), and irradiance (Johnston et al., 2004; Swansburg et al., 2002). $\delta^{13}C$ values are frequently used as proxies for food sources within food web studies (delGiorgio and France, 1996; March and Pringle, 2003). Since phototrophic biofilms can be important food sources within aquatic ecosystems (Bott, 1996; Charlebois and Lamberti, 1996; France, 1996; Boschker et al., 2005) it is important to understand the processes that cause variations in $\delta^{13}C$ within such surface-associated communities Little is known about the factors that influence the $\delta^{13}C$ of phototrophic biofilms but the values are reported to vary with growth rate, irradiance, turbulence, and flow velocity (Trudeau and Rasmussen, 2003; France, 1995a). Turbulence and flow velocity directly influence the CO_2 transport towards a phototrophic biofilm.

In this study we investigated the development of marine and freshwater phototrophic biofilms grown under defined environmental conditions from natural inoculates. We measured the $\delta^{13}C$ values at the different stages in the biofilm development along with

a range of water chemistry and biofilm parameters. The aim of the study was to analyze the variation of the $\delta^{13}C$ during biofilm development and to discuss possible roles of key biotic and abiotic processes for carbon isotope fractionation in photosynthetic biofilms.

2 Methods

Freshwater and marine phototrophic biofilms were grown on removable transparent polycarbonate slides in special designed incubators (Zippel and Neu, 2005), allowing the development of algal dominated biofilms at defined irradiances and flow regimes. Incubators were inoculated with homogenized phototrophic biofilm material. The inoculum material for the freshwater biofilms grew on surfaces in the sedimentation tank of the waste water treatment of Fumicino airport, Rome (Congestri et al., 2005). The marine inoculum material originated from biofilms growing on continuously submerged surfaces in flowing Oosterschelde water, the Netherlands. Inoculation material was mechanically homogenized and then frozen in order to kill fauna and prevent top-down control of the biofilm as much as possible. The fresh-water medium was a modified BG 11-medium (http://www.pasteur.fr/recherche/banques/PCC/Media.htm), with 20 μM silicate to allow diatoms development. The marine biofilms were grown in medium, prepared with commercial available aquarium sea salt (HW Meeressalz Professional, Wiegand, Germany) with additional silicate (20 μM), nitrate (0.35 mM), and phosphate (24 μM).

Medium (4 L per lane) was continuously circulated at flow rates of 25 or 100 l/h in the incubator and refreshed twice a week. The pH of the medium was measured after its preparation with a pH electrode. Biofilms were grown at a range of different growth conditions (Table 1) and the development of the biofilm was followed by a continuous recording of the light attenuation by using 9 light sensors glued on the bottom of several slides along each flow lane. Light attenuation was used as a proxy for the phototrophic biomass at the given growth conditions. Maximum growth rates were estimated by fitting a Richards logistic growth equation (Sidorkewicj et al., 1999) trough the light

attenuation values. The biofilm samples were scraped of the slide and the wet weight was determined for each sample. The samples were freeze dried, dry weight was measured and samples were stored at –80°C until $\delta^{13}C$ analysis. The wet weight of the biofilms was found to increase linearly with light absorption values of up to 80–85% (data not shown).

The $\delta^{13}C$ values were determined at 3 different growth stages during the biofilm development. A first sample was taken 10 days after inoculation (initial phase), the second sample was taken at ~50% light absorption (exponential growth phase) and the third sample was taken at ~90% light absorption (mature or stationary phase). Sampling started close to the outlet site of the incubator to prevent disturbance of biofilms growing on the other slides as much as possible. Sampled slide were replaced by clean slides to prevent additional turbulence, caused by height differences.

2.1 Stable isotope analysis

Biofilm samples were analyzed for natural $\delta^{13}C$ abundance by a total combustion elemental analyzer coupled to an isotope ratio mass spectrometer (IRMS) (Finnigan, germany). Samples were combusted at 1010°C and transported with a helium (5.0 purity) carrier gasflow to the IRMS for determining the isotopic $^{13}C/^{12}C$ ratio of carbon. Stable isotope ratios were calculated as:

$$\delta^{13}C = \left(\frac{\left(\frac{^{13}C}{^{12}C}\right)_{sample}}{\left(\frac{^{13}C}{^{12}C}\right)_{standard}} - 1 \right) \times 1000$$

where the standard is the C-isotope ratio in the Vienna PeeDee Belemnite (0.0112372).

The concentration of total dissolved inorganic carbon in the medium was determined by acidifying 50 ml medium with 500 μl pure phosphoric acid in a closed container (Crimp Seal, Chrompack, the Netherlands) to convert all HCO_3^- and CO_3^{2-} into CO_2. The samples were stored at room temperature to reach equilibrium with the gas phase

(5 ml). 500 μl of the gas phase was injected into a GC with a Poraplot Q column which was linked to the IRMS (Finnigan, Germany) for $\delta^{13}C$ analysis. The CO_2 concentration was calculated using a calibration curve.

Fractionation rate (ε) per phase was calculated as the difference between the average $\delta^{13}C$ of DIC and the $\delta^{13}C$ of the biofilm sampled at that phase. Fractionation was calculated according the equation: $\varepsilon=(\delta^{13}\mathrm{DIC} - \delta^{13}C_{\mathrm{biofilm}})/(1+ \delta^{13}C_{\mathrm{biofilm}}/1000)$ (Freeman and Hayes, 1992). For the initial phase this could be calculated directly, but for the samples from the exponential and mature phase fractionation was calculated as the difference of the average $\delta^{13}C$ of DIC in between the two sampling moments and the $\delta^{13}C$ of the newly formed biomass. The $\delta^{13}C$ of the newly formed biomass was calculated according to $\frac{b_{tn+1}\partial^{13}C_{tn+1}-b_{tn}\partial^{13}C_{tn}}{(b_{tn+1}-b_{tn})}$, where b_{tn} denotes C-biomass at the different sampling moments.

2.2 PLFA-determination

Phospholipid-derived fatty acids (PLFA) originating from cell membranes were used as group specific biomarkers to determine the relative abundance of heterotrophic and phototrophic biomass in the biofilms. PLFA extraction and derivatization was done by an adapted Blyer and Digh protocol (Boschker, 2004). Analysis of the methylated forms of PLFA was done by gas chromatography-flame ionization detection (GC-FID, Interscience, Belgium) using a polar analytical column (Scientific Glass Engineering BPX-70). Biomass contribution of heterotrophic components was estimated by *Chemtax* as described in Dijkman et al. (2006)

2.3 pH microsensor measurement

Three adjacent slides covered with the biofilm were removed from the incubator and positioned into an external flow chamber with fresh medium. The environmental conditions in the external flow chamber (flow, temperature, illumination) were identical to the respective conditions in the biofilm incubator. Glass pH microelectrodes (Glud et

al., 1992) were used to measure depth-profiles of pH in the phototrophic biofilms. The pH microelectrode and a standard calomel reference electrode (Radiometer, Denmark) were connected to a high-impedance millivoltmeter (Keithley, USA). The microsensor was mounted on a motorized micromanipulator (Unisense A/S, Denmark) and depth-profiles were automatically recorded on a PC with a data acquisition system (Profix, Unisense A/S, Denmark). The pH microsensors were calibrated in standard pH buffer solutions of pH 7 and pH 10 (Radiometer, Denmark) and exhibited almost ideal Nernstian response characteristics and a response time of <60 s. The surface position where the pH micro sensor touched the biofilm surface was estimated by visual inspection with a dissection microscope while approaching the sensor tip to the biofilm surface. In order to ensure steady state conditions, the biofilm samples were left in the external flow chamber for 30 min in the light before pH measurements were initiated. Similarly, light was switched off for 30 min before the pH profiles in darkness were acquired.

2.4 Biofilm modeling

Growth and relevant metabolic and geochemical processes in the biofilm were modeled with the *PHOBIA* biofilm kinetic model programmed in Aquasim 2.1 (details in Wolf et al., 2007). The model is a multi-species and multi-substrate mechanistic biofilm model, which has been developed based on the general one-dimensional mathematical biofilm model (Reichert, 1998). It contains kinetics that describes the interactions between photoautotrophic, heterotrophic and chemoautotrophic (nitrifying) functional microbial groups. The biological processes in the model include biomass growth, biomass inactivation and lysis, substrate and nutrient conversion. Growth is estimated as maximum growth rate multiplied by a limitation term, based on the most limiting substrate at the given time points. Light is considered as an energy source and light dependent carbon fixation by phototrophs was modeled via the Eilers and Peeters relationship (Eilers and Peters, 1988), which accounts for light saturation and photoinhibition. Biofilm-specific phenomena are taken into account, such as extracellular polymeric substances (EPS) production by phototrophs as well as gradients of substrates and light in the

biofilm. Acid-base equilibria, in particular carbon speciation, are explicitly accounted for, allowing for the calculation of pH profiles and profiles of the different abiotic carbon species across the biofilm based on chemical acid-base-equilibriums as well as consumption and production terms. The model distinguishes between the usage of different inorganic carbon sources by photoautotrophs, i.e. CO_2 and bicarbonate and combines a number of kinetic mechanisms specific to phototrophic microbial communities, such as internal polyglucose storage under dynamic light conditions, phototrophic growth in the darkness using internally stored reserves, photoadaptation and photoinhibition. We used the same model parameters as Wolf et al. (2007). The settings of the model were based on the measured DIC concentrations and biofilm photosynthesis/respiration rates within the incubator (data not shown).

3 Results

We found minute differences in growth rates between freshwater and marine biofilms. Growth rates at 50% light absorption varied with irradiance, and to a lesser extent, with temperature (Fig. 1) within the chosen conditions. The growth rate was independent with flow rate (data not shown).

The $\delta^{13}C$ values of the different biofilms were measured at three stages of their development. For the freshwater biofilms it was found that $\delta^{13}C$ values became less negative with an increase in biomass (Fig. 2a–e). Changes in $\delta^{13}C$ were strongest for biofilms grown at the highest irradiances. However, the increase was not related to the actual growth rate of the biofilm, which was described well by a logistic growth model. This model implies that the actual growth rate is highest at the initial phase, where after the growth rate decreases with the thickening of the biofilm. At the point where the $\delta^{13}C$ increased, the average growth rate was below the maximum growth rate. The $\delta^{13}C$ values during the development of the marine biofilm showed a contrasting trend (Fig. 3a–e). The $\delta^{13}C$ values during the initial phase were higher (~9‰) than in the freshwater biofilms, but instead of increasing with the thickening of the biofilm, the

values became more negative over time.

Differences in initial DIC concentrations were found between fresh water and salt water medium. The DIC concentrations were 0.34±0.05 mM and 1.5±0.4 mM for freshwater and marine medium, respectively. The $\delta^{13}C$ values of DIC in the media were measured for the two 30°C freshwater runs and for all marine runs. The average differential initial $\delta^{13}C$ value for DIC in freshwater was –10.9±0.8‰ while it was –6.6±1.2‰ in salt water medium. For the runs of which DIC values were measured it was possible to calculate the fractionation rates (ε) per phase (Fig. 4). It was found that fractionation was significantly less in the marine runs (ε=13.1±1.5‰) relative to the fresh water runs (ε=17.5±1.5‰) (anova single factor, $p<0.05$) during growth in the initial phase. No effect of irradiance on fractionation was found during this phase. For the freshwater runs a trend of decreasing fractionation with increasing irradiances was found during the exponential growth phase. This trend was strengthened during the mature phase. However, the fractionation values did not significantly differ between the irradiances during growth in these phases. The marine run showed an increase in fractionation at all irradiances during the exponential phase. In the mature phase this increase continued at 60 μmol photons $m^{-2}\,s^{-1}$. An opposite trend was found for the incubations at 120 μmol photons $m^{-2}\,s^{-1}$. At this irradiance it was found that fractionation decreased during the mature phase. Fractionation values differed significantly (single factor anova (n=3), $p<0.05$) between both irradiances in the mature stage for the marine runs.

The overlaying medium was refreshed twice a week and its pH was measured at refreshment. The pH of renewed freshwater medium was 7.7 while it was 8.1 for the marine medium. It was found that the pH changed within 3 or 4 days during its residence in the incubator. The change in pH was more pronounced at high biofilm biomass and high irradiance (Fig. 5). For one freshwater run and one marine run, additional $\delta^{1}2C$ samples were taken at the end of the run. The reason for the additional sampling was that the pH in the medium changed during the incubation (Fig. 5) affecting the CO_2/HCO_3^- ratio in the overlying water, which may explain the observed variations in $\delta^{13}C$. For this additional sampling, we sampled slides that were put in the incubator as

a replacement of the slides sampled during the course of the run. These low biomass samples (equivalent to the initial phase) were thus incubated in the incubator, while the incubator also contained full grown biofilms. By the additional sampling, the effect of pH changes during the run could be circumvented, since the low biomass samples were incubated in the incubator during a later phase of biomass development, i.e. when the pH change in the medium was most pronounced. The $\delta^{13}C$ values in these additional experiments showed the same trend with biomass development as was found in the other freshwater and marine experiments (Figs. 2e and 3e). However, the effect of light was more pronounced than observed under the normal sampling procedure.

Besides the pH of the medium, pH depth profiles were measured within biofilms, both in the exponential and the mature growth phase (Fig. 6). We only show profiles from one fresh water run and one marine run, which are representative for the other runs. Considerable variation in the biofilm thickness was observed at each growth stage indicating a large spatial heterogeneity of the biofilm structure but the profiles show a consistent and representative view of typical in situ pH characteristics per treatment. In darkness, the pH in the freshwater biofilm matrix did not vary significantly from the pH in the overlaying water, whereas in light the pH clearly increased with depth. This can be taken as an indication of a high CO_2 consumption due to photosynthesis. The increase in pH with depth was most pronounced in the mature biofilms. In addition, a higher irradiance resulted in a more pronounced increase in pH. In marine biofilms it was found that in the dark the pH in the biofilm decreased with depth. In the light an increase was found in the upper part of the biofilm, while at deeper parts the pH decreased again. A decrease in pH can be caused by a net production of CO_2 resulting from high respiratory activity. The increase in pH in the upper part of the biofilm was linked to photosynthetic activity and was strongest at high irradiance.

In order to obtain an indication of the relative contribution of the different microbial groups, PLFA analyses were preformed. Results showed that the bacterial biomass was always highest in the marine runs. The average contribution of bacteria in the marine biofilms was almost twice the value of the freshwater biofilms (Table 2).

BGD
4, 69–98, 2007

3.1 Modeled differences in CO_2 consumption vs. HCO_3^- consumption

In order to explain the variation in $\delta^{13}C$ values found in the freshwater biofilms, we constructed a model describing the chemical and biological processes in a developing freshwater biofilm. The model describes the pH within the biofilm based on charge balance, including the speciation of the different forms of inorganic carbon due to transport, chemical and biological conversion processes. The speciation of the different inorganic C pools was calculated with the model for a freshwater biofilm of 500 μm thickness (Fig. 7a). It was found that at an irradiance of 120 μmol photons m^{-2} s^{-1}, most of the CO_2 was consumed in the upper 150 μm of the biofilm. The HCO_3- pool was much larger than the CO_2 pool and its concentration decreased relatively less with depth. Within the model, CO_2 is preferred above HCO_3^- as carbon source and therefore the CO_2 consumption rate was highest in the top, while in that region almost no HCO_3^- was consumed (Fig. 7b). The significance of HCO_3^- as C-source increased with depth and maximal HCO_3^- consumption was found at 350 μm depth. Below this depth irradiance became limiting and determined the photosynthesis rate rather than the availability of the different inorganic C-pools. With the same model, an estimate of the depth integrated consumption rate of the different inorganic carbon pools during the biomass development was calculated (Figs. 8a+b). It was found that initially CO_2 was the most important C- source for carbon fixation. With increasing thickness of the biofilm the relevance of CO_2 for total photosynthesis decreased. For >400 μm thick biofilms, HCO_3^- eventually became the most important C-source for photosynthesis (Fig. 8b).

4 Discussion

We will start the discussion with the freshwater system, where we observed that $\delta^{13}C$ values varied with the development of phototrophic biofilms. In the initial growth phase no clear correlation was found between $\delta^{13}C$ values and the growth rate or irradiance,

indicating that the biofilm growth rate did not affect isotopic fractionation rates. This is in contrast with relationships found for isotope fractionation in phytoplankton, where several studies showed that the growth rate (Fry and Wainright, 1991; Laws et al., 1995; Rau et al., 1996), and irradiance (Rost et al., 2002) had an inverse relationship with isotopic fractionation in different phytoplankton species. The rationale behind this expected inverse correlation is that at high growth rates RUBISCO becomes transport limited for CO_2 resulting in: 1) under saturation of RUBISCO and therefore a lower fractionation, or 2) a shift from CO_2 to HCO_3^- as the most important C-source. Both cases will lead to increasing $\delta^{13}C$ values.

It can be assumed that irradiance determines growth during the initial stage, and that no other substrate than light is limiting at this stage. A correlation between the relative growth rate at 50% absorbance and irradiance was found (Fig. 1); logistic growth models describe that growth rates are highest during the initial phase. During this phase, the $\delta^{13}C$ values were lowest. As soon as the availability of any substrate becomes limiting for growth, the net biofilm growth rate will decrease during further development. After this onset of limitation, we found increasing $\delta^{13}C$ values and a decrease in fractionation in the freshwater biofilms indicating that the diffusive transport of $CO_{2(aq)}$ became limiting in the biofilm during the later developmental stages.

Due to methodological limitations we were only able to measure the $\delta^{13}C$ value at the whole biofilm level and not on cellular level. In free-living phytoplankton, population-based results may closely reflect the average of individual cells, but in our biofilm communities we could only measure the depth integrated value. Our model showed that the concentration of the different C-sources is not homogenously distributed with depth and that the depth integrated net-C fixation becomes increasingly C-limited with the thickening of the biofilm, especially since little heterotrophic biomass is found in our freshwater biofilms. Low heterotrophic biomass cannot provide intensive carbon recycling of photosynthetic products during the light period.

Variations of $\delta^{13}C$ values in biofilms may be due to changes in C-source rather than being solely the result of limited $CO_{2(aq)}$ availability. We found a fractionation

of ~13–17‰ in the initial stage of biofilm growth, and the modeled C-concentrations and volumetric C-fixation rates were relatively high, both indicating that $CO_{2(aq)}$ was not limiting at that stage of biofilm formation (Fig. 7). In a 500 μm thick biofilm, it was shown by the model that the top layer (<70 μm) was not limited by $CO_{2(aq)}$ at an irradiance of 120 μmol photons m^{-2} s^{-1}.

During further growth of the biofilm, model calculations showed that despite decreasing biofilm growth and volumetric C-consumption rates, the depth integrated areal C-fixation rate increased causing a shift from CO_2 towards HCO_3^- as the most important C-source for photosynthesis. This shift explains the progression towards less negative $\delta^{13}C$ values we observed in thick freshwater biofilms. We also found that the difference in $\delta^{13}C$ between the initial and stationary biofilm growth phase became larger at higher irradiances. The opposite trend was found for fractionation at the different irradiances (less fractionation at higher irradiances). Biofilm thickness was approximately similar (light absorption determined the moment of sampling) for all sampled irradiances at each given sampling event. Therefore we conclude that for fully matured, stationary-phase biofilms (no net growth) a correlation can be found between depth integrated photosynthesis rate and $\delta^{13}C$ values.

Our data showed no correlation between the $\delta^{13}C$ value and flow rate, although relationships between fractionation and mass transport or flow velocity are well described for phototrophic biofilms (France, 1995a; Larned et al., 2004; France, 1995b). However, these studies may have complete different flow regimes. Our system was developed to have linear flow characteristics with as little turbulence as possible, which was different from the system described by France (1995) and Larned et al. (2004). Turbulence might affect biofilm development differently.

A reason for the absence of the relationship with flow velocity in our system may be that in the initial, or exponential growth phase of biofilms, mass transfer limitation is not an issue. Thinner diffusive boundary layers, as a result of higher flow rates or turbulence levels during this phase will not affect fractionation efficiencies for $^{13}CO_2$ by RUBISCO since CO_2 availability is not a limiting factor for fractionation. From the

same line of reasoning as was used for the growth rate (see above), it can be argued that a correlation between flow rate or turbulence and $\delta^{13}C$ value will only be found under diffusion limited conditions, i.e. late exponential and mature biofilms. In natural systems it will be difficult to distinguish and sample from the different stages of the biofilm development, since heterogeneity in developmental stages are present on a small spatial scale, due to sloughing, grazing, etc (Biggs, 1996; Havens et al., 1996).

Growth rates of the marine biofilms did not differ from the freshwater biofilms but we found an opposite trend between biomass and $\delta^{13}C$ values (Fig. 3). In addition, the $\delta^{13}C$ value of the DIC was 7‰ less negative than in the fresh water medium. This difference in $\delta^{13}C$ value of the DIC can explain part of the difference of the initial $\delta^{13}C$ of the marine biofilms, but part of the difference was explained by differences in fractionation during the initial phase. However, neither the initial $\delta^{13}C$ value of the DIC, nor the lower $CO_{2(aq)}$ explains the decrease in $\delta^{13}C$ value with the thickening of the biofilms. A decrease in $\delta^{13}C$ values may be explained by the expected decrease in growth rate with the thickening of the biofilm, as has been shown for phytoplankton species (Fry and Wainright, 1991; Laws et al., 1995; Rau et al., 1996). However, from the measured pH and DIC concentrations it was calculated that the initial $CO_{2(aq)}$ concentration in the marine medium was approximately 3–4 times lower than the freshwater medium despite the higher DIC concentrations. Therefore, it is likely that the marine biofilms were more limited in $CO_{2(aq)}$ than the freshwater biofilms, and this should eventually lead to an even stronger relationship between biomass and $\delta^{13}C$ values in the marine biofilms as compared to the freshwater biofilms.

In our experiments, one clear difference between the freshwater and the marine biofilms was that heterotrophic biomass was twice as high in the marine biofilms. Higher heterotrophic biomass is assumed to result in a higher recycling of carbon within the biofilm and as a result increase the availability of $CO_{2(aq)}$. A lowering of the pH with depth in the dark, indicative for a high respiratory activity, was indeed found in the marine biofilms. A decrease in pH with depth in the dark was almost absent in the freshwater system and as a result we conclude that a much higher heterotrophic ac-

tivity was present within the marine biofilms in our system. This was also confirmed from oxygen microprofile measurements (data not shown). Carbon cycling within a biofilm may reduce the $\delta^{13}C$ value. It has been shown that as soon as ecosystems shift from phototrophic towards heterotrophic systems this will lower the $\delta^{13}C$ values (Schindler et al., 1997; Bade et al., 2004). High respiration rates will increase the heterotrophy level of the biofilm and elevate the CO_2 cycling and its availability for the phototrophic organisms. Moreover, respiration enriches mostly the $^{12}CO_2$ pool since its source (biomass) is lighter, relative to the DIC pool.

In conclusion, we found that the $\delta^{13}C$ value depends on the development phase of the photosynthetic biofilm as well as on environmental conditions, and fractionation seems to be correlated with biofilm thickness or net depth-integrated photosynthesis rates rather than with the biofilm growth rate. The direction in which the $\delta^{13}C$ value develops during biomass accretion depends on two factors: 1) the net depth-integrated C-fixation and 2) the recycling of C driven by heterotrophic activity. In our system, a difference in heterotrophic activity most likely resulted in completely different trends of $\delta^{13}C$ values with biofilm thickness in the freshwater and the marine biofilms. We cannot conclude whether heterotrophic recycling is always more important in marine systems than in fresh water systems, but at least in our system it was. This difference was found across different independently grown inoculums used to seed biomass in the different runs. Since surface-associated microalgae and cyanobacteria are amongst the most successful and efficient primary producers in benthic aquatic environments, and are considered a main source of energy for higher trophic levels in natural systems, such trends in $\delta^{13}C$ values need to be taken into account if $\delta^{13}C$ value are used for food web studies.

Acknowledgements. A. Glud is thanked for manufacturing the pH microelectrodes. Paul v. d. Berg and S. Jensen are thanked for running the incubators and assistance with the data collection. This work was financed by the European Union, PHOBIA, EU contract QLRT-2001-01938, and the Danish Natural Science Research Council (RT and MK). This is publication nr 3990 of NIOO-CEME.

References

Bade, D. L., Carpenter, S. R., Cole, J. J., Hanson, P. C., and Hesslein, R. H.: Controls of delta C-13-DIC in lakes: Geochemistry, lake metabolism, and morphometry, Limnnol. Oceanogr., 49(4), 1160–1172, 2004.

Biggs, B. J. F.: Patterns in benthic aglae of streams. Algal Ecology: Freshwater Benthic Ecosystems, edited by: Stevenson, R. J., Bothwell, M. L., and Lowe, R. L., San Diego, Academic Press, 31–56, 1996.

Boschker, H. T. S.: Linking microbial community structure and functioning: stable isotope (13C) labeling in combination with PLFA analysis. Molecular Microbial Ecology Manual II, edited by: Kowalchuk, G. A., de Bruijn, F. J., Head, I. M., Akkermans, A. D., and van Elsas, J. D.: Dordrecht, The Netherlands, Kluwer Academic Publishers, 1673–1688, 2004.

Boschker, H. T. S., Kromkamp, J. C., and Middelburg, J. J.: Biomarker and carbon isotopic constraints on bacterial and algal community structure and functioning in a turbid, tidal estuary, Limnnol. Oceanogr., 50(1), 70–80, 2005.

Bott, T. L.: Algae in microscopic food webs. Algal Ecology: Freshwater Benthic Ecosystems, edited by: Stevenson, R. J., Bothwell, M. L., and Lowe, R. L., San Diego, Academic Press, 574–609, 1996.

Cassar, N., Laws, E. A., Bidigare, R. R., and Popp, B. N.: Bicarbonate uptake by Southern Ocean phytoplankton, Glob. Geochem. Cyc., 18(2), 1–10, 2004.

Charlebois, P. M. and Lamberti, G. A.: Invading crayfish in a Michigan stream: Direct and indirect effects on periphyton and macroinvertebrates, J. N. Am. Benthol. Soc., 15(4), 551–563, 1996.

Congestri, R., Cox, E. J., Cavacini, P., and Albertano, P.: Diatoms (Bacillariophyta) in phototrophic biofilms colonising an italian wastewater treatment plant, Diatom Res., 20(2), 241–255, 2005.

Decho, A. W.: Microbial biofilms in intertidal systems: an overview, Cont. Shelf Res., 20(10–11), 1257–1273, 2000.

delGiorgio, P. A. and France, R. L.: Ecosystem-specific patterns in the relationship between zooplankton and POM or microplankton delta C-13, Limnol. Oceanogr., 41(2), 359–365, 1996.

Dijkman, N. A. and Kromkamp, J. C.: Phospholipid-derived fatty acids as chemotaxonomic markers for phytoplankton: application for inferring phytoplankton composition, Mar. Ecol.

-Prog. Ser., 324, 113–125, 2006.
Eilers, P. H. C. and Peeters J. C. H.: A Model for the Relationship between Light-Intensity and the Rate of Photosynthesis in Phytoplankton, Ecolog. Model., 42(3–4), 199–215, 1988.
France, R. L.: Differentiation between littoral and pelagic food webs in lakes using stable carbon isotopes, Limnol. Oceanogr., 40(7), 1310–1313, 1995a.
France, R. L.: C-13 enrichment in benthic compared to planktonic algae – foodweb implications, Mar. Ecol.-Prog. Ser., 124(1–3), 307–312, 1995b.
France, R. L.: Stable isotopic survey of the role of macrophytes in the carbon flow of aquatic foodwebs, Vegetatio, 124(1), 67–72, 1996.
Freeman, K. H. and Hayes J. M.: Fractionation of carbon isotopes by phytoplankton and estimates of ancient CO2 levels, Glob. Biogeochem. Cycles 6, 185–198, 1992.
Fry, B. and Wainright, S. C.: Diatom sources of C-13-rich carbon in marine food webs, Mar. Ecol.-Prog. Ser., 76(2), 149–157, 1991.
Glud, R. N., Ramsing, N. B., and Revsbech, N. P.: Photosynthesis and photosynthesis-coupled respiration in natural biofilms quantified with oxygen microsensors, J. Phycol., 28(1), 51–60, 1992.
Goericke, R., Montoya, J. P., and Fry, B.: Physiology of isotopic fractionation in algae and cyanobacteria. Stable isotopes in ecology and environmental science, edited by: Lajtha, K. and Michener, R. H, London, Blackwell Scientific Publications, 187–221, 1994.
Havens, K. E., East, T. L., Meeker, R. H., Davis, W. P., and Steinman, A. D.: Phytoplankton and periphyton responses to in situ experimental nutrient enrichment in a shallow subtropical lake, J. Plankton Res., 18(4), 551–566, 1996.
Hayes, J. M.: Factors controlling C-13 contents of sedimentary organic-compounds – Principles and evidence, Mar. Geol., 113(1–2), 111–125, 1993.
Johnston, N. T., MacIsaac, E. A., Tschaplinski, P. J., and Hall, K. J.: Effects of the abundance of spawning sockeye salmon (*Oncorhynchus nerka*) on nutrients and algal biomass in forested streams, Can. J. Fish. Aquat. Sci., 61(3), 384–403, 2004.
Larned, S. T., Nikora, V. I., and Biggs, B. J. F.: Mass-transfer-limited nitrogen and phosphorus uptake by stream periphyton: A conceptual model and experimental evidence, Limnnol. Oceanogr., 49(6), 1992–2000, 2004.
Laws, E. A., Popp, B. N., Bidigare, R. R., Kennicutt, M. C., and Macko, S. A.: Dependence of phytoplankton carbon isotopic composition on growth-rate and $[CO_2](Aq)$ – theoretical considerations and experimental results, Geochim. Cosmochim. Ac., 59(6), 1131–1138, 1995.

Lewis, M. A., Weber, D. E., Goodman, L. R., Stanley, R. S., Craven, W. G., Patrick, J. M., Quarles, R. L., Roush, T. H., and Macauley, J. M.: Periphyton and sediment bioassessment in north Florida Bay, Environ. Monit. Assess., 65(3), 503–522, 2000.

March, J. G. and Pringle, C. M.: Food web structure and basal resource utilization along a tropical island stream continuum, Puerto Rico, Biotropica, 35(1), 84-93, 2003.

Rau, G. H., Riebesell, U., and WolfGladrow, D.: A model of photosynthetic C-13 fractionation by marine phytoplankton based on diffusive molecular CO_2 uptake, Mar. Ecol-Pog. Ser., 133(1–3), 275–285, 1996.

Raven, J. A.: Phylogeny, palaeoatmospheres and the evolution of phototrophy. Stable Isotopes Integration of biological, ecological and geochemical processes, edited by: Griffiths, H., Oxford, Bios Scientific Publishers Limited, 323-341, 1998.

Roeske, C. and O'Leary, M.: Carbon isotope effect on carboxylation of ribulase biphospahte catalyzed by ribulase biphosphate carborxylase from *Rhodospirillum rubrum*, Biochemistry, 24, 1603–1607, 1985.

Rost, B., Zondervan, I., and Riebesell, U.: Light-dependent carbon isotope fractionation in the coccolithophorid *Emiliania huxleyi*, Limnol. Oceanogr., 47(1), 120–128, 2002.

Schindler, D. E., Carpenter, S. R., Cole, J. J., Kitchell, J. F., and Pace, M. L.: Influence of food web structure on carbon exchange between lakes and the atmosphere, Science, 277(5323), 248–251, 1997.

Sidorkewicj, N. S., Lopez Cazorla, A. C., Fernandez, O. A., Mockel, G. C., and Burgos, M. A.: Effects of Cyprinus carpio on Potamogeton pectinatus in experimental culture: the incidence of the periphyton, Hydrobiologia, 415, 13–19, 1999.

Stumm, W. and Morgan, J. J.: Aquatic chemistry: Chemical equilibria and rates in natural waters, NEW YORK, Wiley-Interscience, 1995.

Swansburg, E. O., Fairchild, W. L., Fryer, B. J., and Ciborowski, J. J. H.: Mouthpart deformities and community composition of chironomidae (diptera) larvae downstream of metal mines in New Brunswick, Canada. Environ. Toxicol. Chem., 21(12), 2675–2684, 2002.

Tortell, P. D. and Morel, F. M. M.: Sources of inorganic carbon for phytoplankton in the eastern Subtropical and Equatorial Pacific Ocean, Limnnol. Oceanogr., 47(4), 1012–1022, 2002.

Trudeau, V. and Rasmussen, J. B.: The effect of water velocity on stable carbon and nitrogen isotope signatures of periphyton, Limnol. Oceanogr., 48(6), 2194–2199, 2003.

Werne, J. P. and Hollander, D. J.: Balancing supply and demand: controls on carbon isotope fractionation in the Cariaco Basin (Venezuela) Younger Dryas to present, Mar. Chem., 92(1–

4), 275–293, 2004.
Wolf, G., Picioreanu, C., and van Loosdrecht, M. C. M.: Kinetic modelling of phototrophic biofilms – the PHOBIA model., Water Resour. Res., in press, 2007.
Zippel, B. and Neu, T. R.: Growth and structure off phototrophic biofilms under controlled light conditions, Water Sci. Technol., 52(7), 203–209, 2005.

Table 1. Growth conditions in the incubator at the different incubations.

medium	Temperature (°C)	Flow rate (l/h)	Irradiance (μmol photons m^{-2} s^{-1})
Fresh	20	25	15, 30, 60 and 120
		100	
	30	25	
		100	
Marine	15	25	
		100	
	25	25	
		100	

Table 2. Percentage of heterotrophic biomass relative to the total biomass present in the different treatments based on chemtax analysis of the PLFA determination.

Medium	Temperature	flow	Irradiance μmol photons m^{-2} s^{-1}			
			120	60	30	15
Freshwater	20	25	7	5	15	8
		100	2	8	15	ND
	30	25	2	6	6	ND
		100	5	2	2	ND
average		4	5	10	8	
saltwater	15	25	6	11	11	ND
		100	18	15	17	19
	25	25	15	23	19	58
		100	22	36	44	ND
average		15	21	23	39	

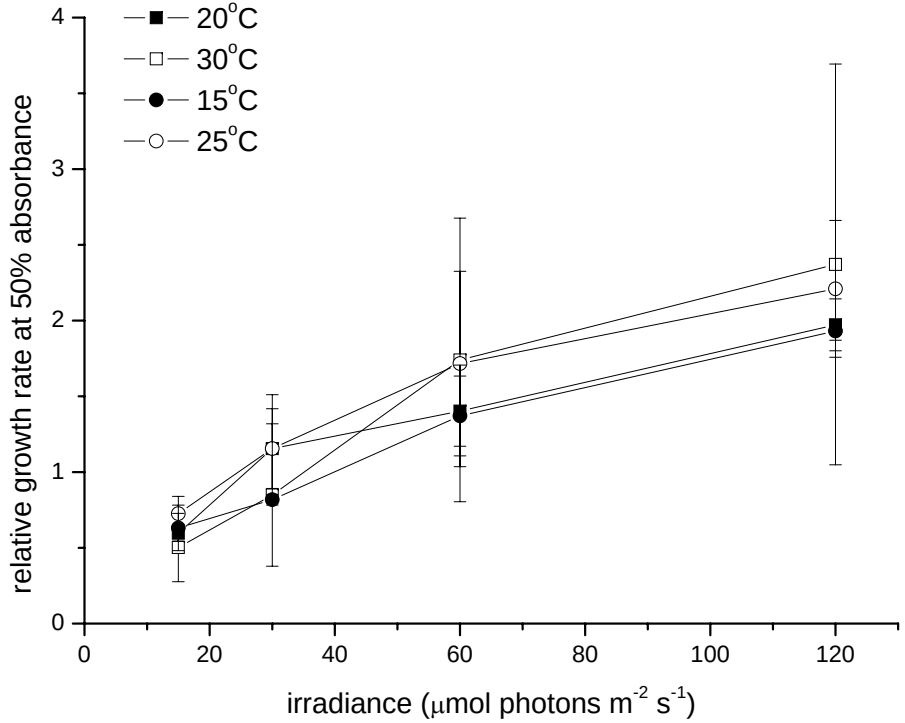

Fig. 1. Average maximum growth rates at different irradiances in freshwater (squares) and marine (circles) media. The maximum growth rates were estimated using a logistic growth model. Incubation temperatures are indicated in the graph.

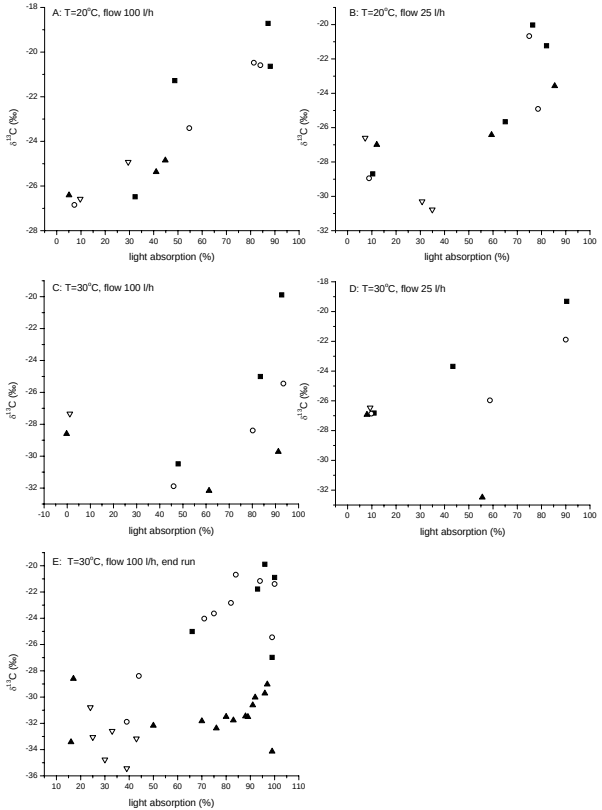

Fig. 2. Development of δ^{13}C values in developing freshwater phototrophic biofilms. **(a)**–**(d)** show the relationship of δ^{13}C values with biomass per treatment (temperature and flow rate are indicated in the graphs). Biomass is expressed as light absorption. **(e)**: δ^{13}C value samples taken at the end of the run to overcome the effects in changes in pH in the medium. Symbols indicate different irradiances 120 μmol photons $m^{-2}\,s^{-1}$(closed squares), 60 μmol photons $m^{-2}\,s^{-1}$ (open circles), 30 μmol photons $m^{-2}\,s^{-1}$ (closed triangles) and 15 μmol photons $m^{-2}\,s^{-1}$ (open triangles).

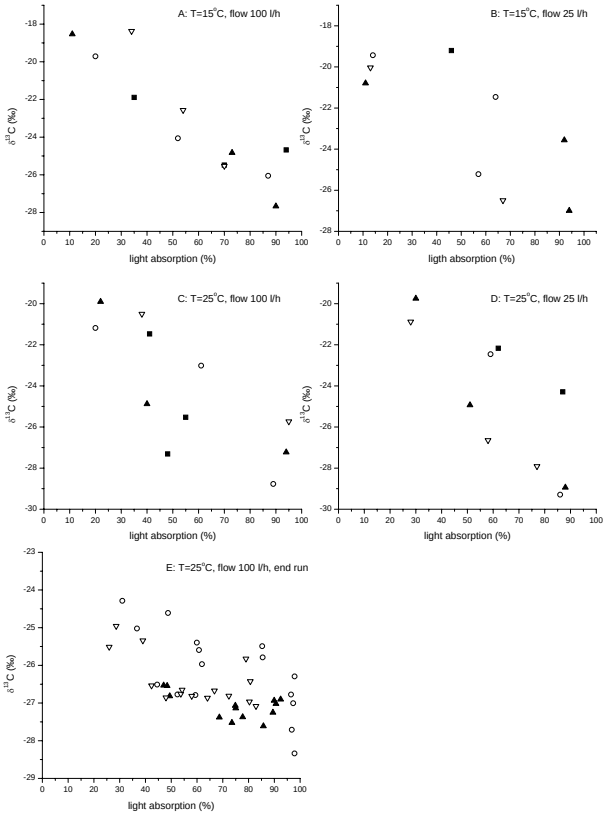

Fig. 3. Development of $\delta^{13}C$ values in developing marine phototrophic biofilms. **(a)–(d)** show the relationship of $\delta^{13}C$ values with biomass per treatment (temperature and flow rate are indicated in the graphs). Biomass is expressed as light absorption. **(e)**: $\delta^{13}C$ value samples taken at the end of the run to overcome the effects in changes in pH in the medium. Symbols indicate different irradiances 120 μmol photons m^{-2} s^{-1}(closed squares), 60 μmol photons m^{-2} s^{-1} (open circles), 30 μmol photons m^{-2} s^{-1} (closed triangles) and 15 μmol photons m^{-2} s^{-1} (open triangles).

BGD
4, 69–98, 2007

EGU

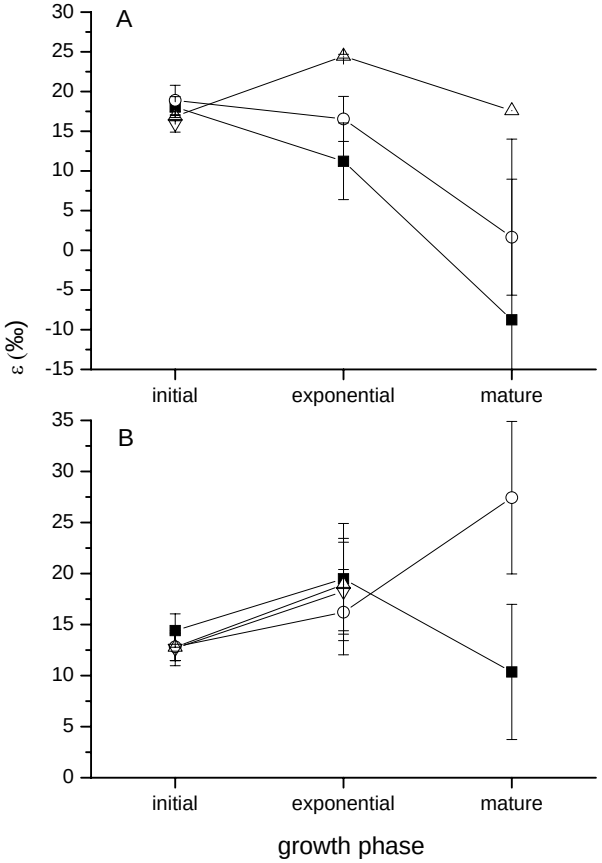

Fig. 4. Average fractionation (ε) per irradiance during the three growth phases throughout the development of phototrophic biofilms. Biofilms were grown at incident photon fluxes of 120 (black squares), 60 (open circles), 30 (up triangles) and 15 (down triangles). The average values and error bars were calculated over successively 2 (freshwater, graph **a**) and 4 (marine, graph **b**) separate runs.

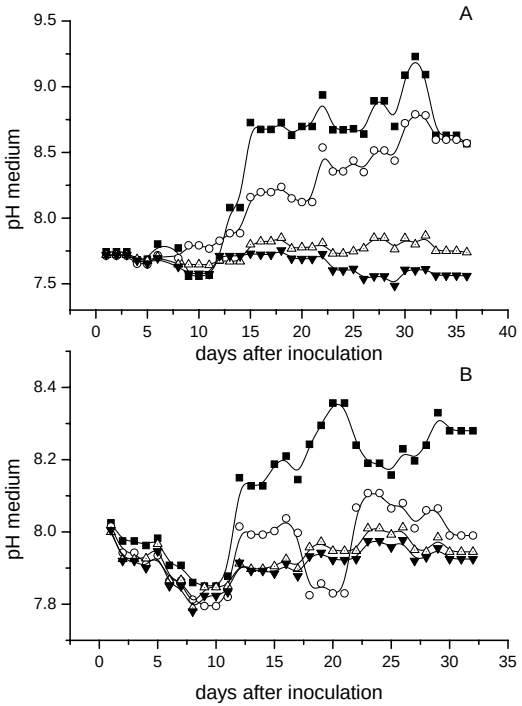

Fig. 5. Averaged pH of the overlaying growth medium (n=5) during the development of phototrophic biofilms grown at different irradiances and media. The media was refreshed twice a week, and the pH was assumed to be stable after half a day of incubation. The highest standard deviations were found in the 120 μmol photons m^{-2} s^{-1} treatment. The average standard deviations at that irradiance were 0.55 and 0.19 for respectively the freshwater and marine runs. The maximum standard deviations of these runs were respectively 0.95 and 0.35. The different incubation irradiances were 15 (gray triangles), 30 (open triangles), 60 (closed circles) and 120 μmol photons m^{-2} s^{-1} (open squares).

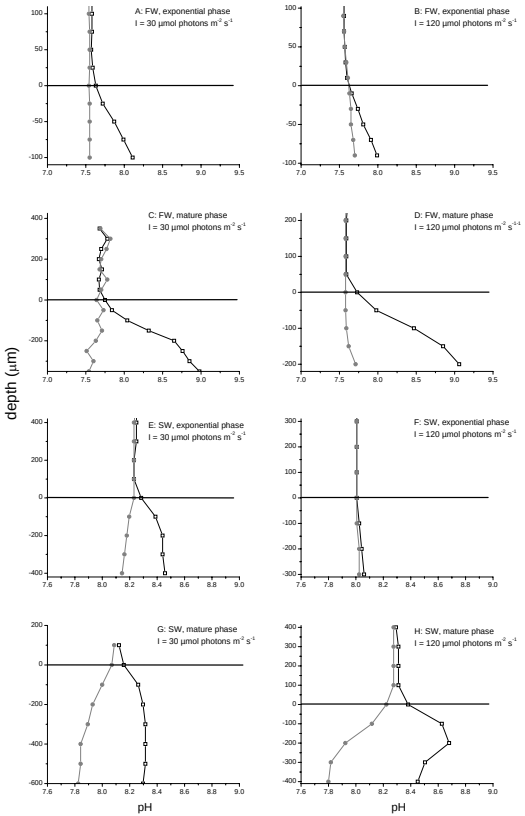

Fig. 6. pH micro profiles measured in biofilms of the exponential (**a, b, e** and **f**) and mature phase (**c, d, g** and **h**) in a freshwater (FW) at 30˚C (a–d) and a marine (SW) biofilm at 25˚C (e–g) at 100 l/h flow. The biofilms have been grown at two irradiances: 30 (a, c, e and g) and 120 μmol photons m^{-2} s^{-1} (b, d, f and h). Open circles represent pH profiles measured in the dark, closed squares represent pH profiles measured in the light.

BGD
4, 69–98, 2007

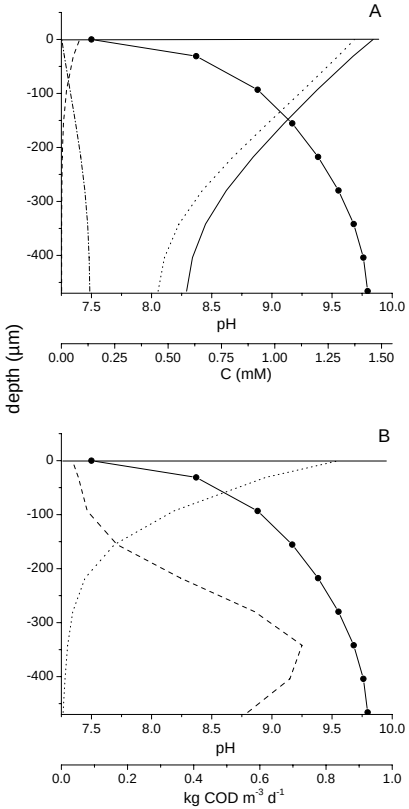

Fig. 7. (a) Modeled distribution of the C-species: CO_2 (dashed line), HCO_3^- (dotted line), CO_3 (dash dotted line) and total inorganic C (solid line) over depth at 120 μmol photons $m^{-2}\,s^{-1}$ in a biofilm of ~470 μm thick. The pH is also expressed (closed circles). **(b)** Modeled carbon consumption rate with depth in a biofilm of ~470 μm thick, at an irradiance of 120 μmol photons $m^{-2}\,s^{-1}$. Total inorganic carbon consumption is separated in a consumption rate of $CO_{2(aq)}$ (dashed line) and HCO_3 (dotted line).

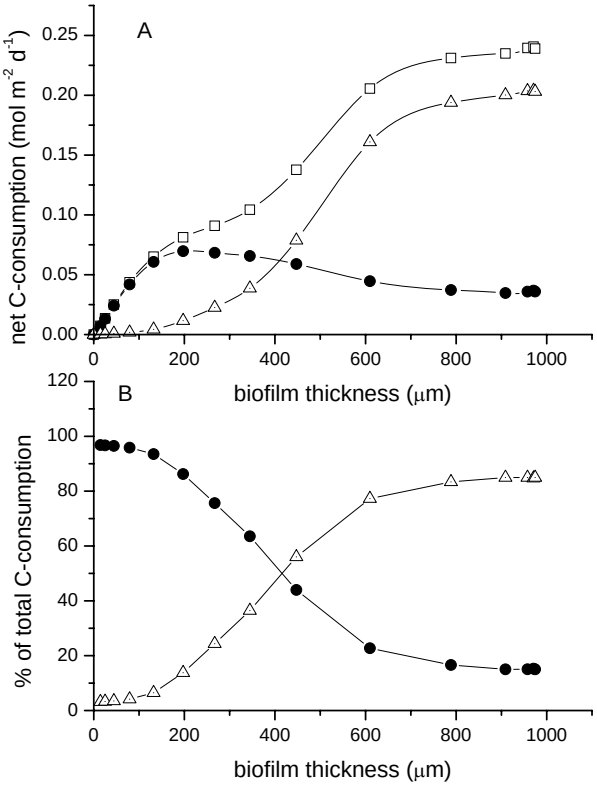

Fig. 8. Relationship between depth integrated C-consumption with the biomass development (biofilm thickness) based on a mechanistic model describing phototrophic biofilm growth **(a)**: net-total inorganic C consumption (squares), CO_2consumption (circles) and HCO_3^- consumption (triangles). The lower graph **(b)** indicates the shift in contribution from CO_2 (closed circles) to HCO_3^- (open triangles) to the total C-consumption.